http://dx.doi.org/10.5012/bkcs.2012.33.4.1177

Electrochemical Properties of NiO-YSZ Thin Films on 316 Stainless Steel Bipolar Plates Under a Simulated PEMFC Environment

W. G. Lee and H. Jang*

*Department of Materials Science and Engineering, Korea University, Seoul 136-713, Korea. *E-mail: hojang@korea.ac.kr*
Received November 16, 2011, Accepted December 30, 2011

The corrosion resistance of 316L stainless steel coated with NiO-YSZ (Ni added yttria stabilized zirconia) was examined in a proton exchange membrane fuel cell (PEMFC) environment. The NiO-YSZ coating was carried out using a sol-gel dip coating method, and the corrosion resistance and interfacial contact resistance (ICR) were determined by the composition and morphology of the NiO-YSZ film. The corrosion resistance increased with increasing Ni content in the NiO-YSZ film, but rapid corrosion was observed when the YSZ film contained more than 15 wt % Ni due to surface cracks. The polarization resistance was improved by several orders of magnitude when 316L stainless steel was coated with a 15 wt % NiO-YSZ film compared to bare 316L. The ICR of the NiO-YSZ film was decreased to that of bare 316L when the YSZ film contained 25 wt % NiO, suggesting the possible application of NiO-YSZ coated stainless steel for a bipolar plate.

Key Words : Ni, YSZ, Sol-gel, Metallic bipolar plate, PEMFC

Introduction

The bipolar plate used in proton exchange membrane fuel cells (PEMFCs) is a multifunctional component because it electrically connects the cells in series, separates the gases in the adjacent cells, and accommodates the gas flow channels. Therefore, bipolar plates need to be electrically conducting, mechanically strong, and resistant to corrosion.[1] Currently, graphite bipolar plates are used widely for commercial PEMFC (proton exchange membrane fuel cell) assemblies because graphite is electrically conducting, chemically stable, and easy to fabricate. On the other hand, the graphite bipolar plate, which is brittle and porous, needs to be a few millimeters thick to support the membrane electrode assembly (MEA), which increases the weight and volume of the stack.[1,2]

Several candidates for bipolar plates have been developed to replace the graphite plate. These are based on metals and composite materials, mainly concerning the reduction of the stack size and longer service life. Metal alloys have attracted recent attention owing to their good thermal and electrical conductivity and easy fabrication *via* stamping or etching to produce channels for the reactant and product gases. Another advantage of metal plates is their low gas permeability, which allows thin plates and a decrease in stack volume.[3,4] Metallic bipolar plates, however, have low corrosion resistance compared to graphite and carbon composites due to the possible acid leaching from the MEA in the PEMFC.[2-9] A range of surface modifications, such as thermal nitriding, TiN coating, polymer coating, carbon coating and diffusion coating, have been carried out to protect the metallic bipolar plates from corrosion.[10,11] Nevertheless, they are seldom used as bipolar plates in a commercial PEMFCs due to their low mechanical properties or high manufacturing cost.

Another possible surface modification for the metallic bipolar plate is a sol-gel coating to produce corrosion resistant and electrically conducting films on the metal surface. The sol-gel process has advantages over other traditional methods in terms of equipment, processing and manufacturing cost. Another benefit of employing the sol-gel method is the good adhesion of the film to the substrates,[12-14] providing excellent protection from oxidation and acid attack.[12,15] Among the materials coated by the sol-gel method, zirconia or yttria-stabilized zirconia (YSZ) has several advantages, such as good corrosion resistance, high mechanical strength, chemical durability and thermal expansion coefficient comparable to various metals.[16-21] On the other hand, zirconia and YSZ films produced on metal substrates by sol-gel processes have high interfacial contact resistance and are unacceptable as a bipolar plate.[22] This is because high electrical conductivity is one of the key requirements for commercial PEMFC bipolar plates.[2,23-25]

In the present study, YSZ modified by nickel oxide was coated on a stainless steel plate to improve the properties required for PEMFC bipolar plates. Ni was added to the YSZ film in the course of the sol-gel processing to reduce the ICR because bipolar plates require corrosion resistance and a low ICR. To examine the corrosion resistance of 316L stainless steel coated with a NiO-YSZ film, potentiodynamic tests were carried out under PEMFC operating conditions, while the ICR value was measured as a function of the contact force.

Experimental Details

A commercially available 316L austenitic stainless steel sheet was used as the substrate for the sol-gel coating. Table 1 lists the composition of the steel. The sheet was 2 mm thick and was cut into 16 mm diameter discs for the sol-gel

Table 1. Chemical composition of 316L stainless steel (wt %)

Cr	Ni	Mo	Mn	S	Si	C	P	Fe
16.00-18.00	10.00-14.00	2.00-3.00	2.00↓	0.030↓	0.75↓	0.03↓	0.045↓	Balance

coating and subsequent corrosion tests. Before the coating, the specimens were polished with #2000 SiC abrasive papers and degreased ultrasonically with acetone.

Three different precursors; $ZrO(NO_3)_2{\cdot}2H_2O$ (Sigma Aldrich), $Y(NO_3)_3{\cdot}6H_2O$ (Sigma Aldrich), and $Ni(NO_3)_2{\cdot}6H_2O$ (Sigma Aldrich), were diluted in ethanol (C_2H_5OH) to produce a solution for the sol-gel coating. The fraction of $(NiO_3)_2{\cdot}6H_2O$ in the solution was changed to obtain different Ni concentrations in the final NiO-YSZ film. The solution was homogenized with a magnetic stirrer for an hour at room temperature until it became transparent. The 316L stainless steel substrate was soaked completely in the solution, pulled out at 5 cm/sec, and dried at room temperature for 1 hour. The dried samples were calcined for 1 hour in a tube furnace at 800 °C under an argon atmosphere.

The structure of the NiO-YSZ film was examined by X-ray diffraction (XRD, Rigaku D/MAX-2500V/PC) using Cu-K_α radiation (λ = 1.54 Å). The surface morphology of the film was examined by scanning electron microscopy (SEM, Hitachi S-4300) and the compositional depth profile was obtained by auger electron spectroscopy (AES, PHI 680). The surface roughness was measured by laser confocal microscopy (Wyko NT1100, Veeco Inst. Inc.).

The potentiodynamic tests were carried out using a computerized potentiostat (VMP3-CHAZ, Princeton Applied Research) to evaluate the electrochemical response of the bare and NiO-YSZ coated 316L stainless steels. The corrosion circuit consisted of three electrodes; a graphite counter electrode, a saturated calomel electrode as a reference electrode, and a stainless steel specimen as the working electrode. To simulate the PEMFC operation conditions, the corrosion tests were carried out in a 1 M H_2SO_4 + 2 ppm F^- solution at 70 °C. Sulfuric acid was used for the corrosion evaluation to mimic the acidic polymer electrolyte. A relatively aggressive solution was employed to accelerate the corrosion reaction.

The ICR measurement was carried out according to Davies' method.[6] The voltage drop across the specimen located in the middle of two copper plates was measured as a function of the force up to 500 N.[3,10,11] Two pieces of conducting carbon paper were inserted between the sample plate and copper plates. An electrical current (1A) was provided through the two copper plates. The ICR was monitored using an Agilent 34401A potentiometer. Before the ICR test, the 316L specimens were polished with #800 SiC abrasive paper.

Results and Discussion

Structure and Surface Morphology of the NiO-YSZ Film. The crystal structure of the NiO-YSZ film coated on the stainless steel was examined by XRD (Fig. 1). The XRD pattern shows two sets of peaks; one set from the austenitic stainless steel phase, and the other set from the NiO-YSZ layer, which comprises tetragonal zirconia, cubic Y_2O_3, and cubic NiO phases. The figure clearly indicates the appearance of the NiO peaks when the film contains Ni. The composition of the YSZ film was also examined by AES (Fig. 2). The depth profiles show Fe, Cr, Zr, C, Ni and O as a function of the sputtering time. Yttrium was not detected due to the small amount in the precursor. On the other hand, the thickness of the film obtained in the depth profiles of the all samples was from 404.6 nm to 975.8 nm as a function of Ni content in the NiO-YSZ film, as the sputtering rate of a standard specimen under the same conditions was approximately 23.8 nm/min.

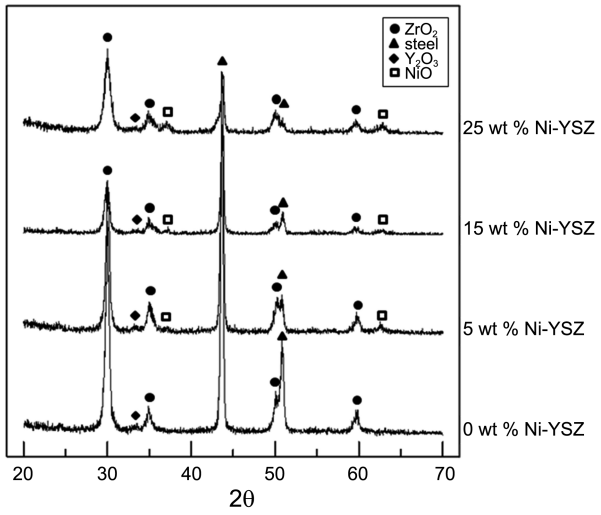

Figure 1. X-ray diffraction patterns of NiO-YSZ coated stainless steel showing the peaks from 316L stainless steel, zirconia, Y_2O_3, and NiO.

The surface of the film was examined by SEM because the final surface roughness or other artifacts, such as microcracks and pores, can affect the performance of the bipolar plates. Figure 3 shows the film surface when it contains 0 to 25 wt % Ni. The NiO-YSZ film was well adhered and uniform without showing cracks or pores up to 15 wt % of NiO in the film. On the other hand, microcracks appeared in the film containing more than 15 wt % NiO (Fig. 3(c) and (d)), indicating that Ni increased the stress on the film during cooling after heat treatment. This is an interesting finding because the Ni oxide in the YSZ film was expected to not only decrease the ICR of the film but also relieve the stress at the interface between the 316L substrate and YSZ film. This is because the thermal expansion coefficient of NiO (α = 12.1 × 10^{-6}/°C) is greater than that of YSZ (α = 10.05 × 10^{-6}/°C) but smaller than 316L stainless steel (α = 16.2 × 10^{-6}/°C). On the other hand, the stress relieving effect of NiO was not observed. The main cause of the microcracks in

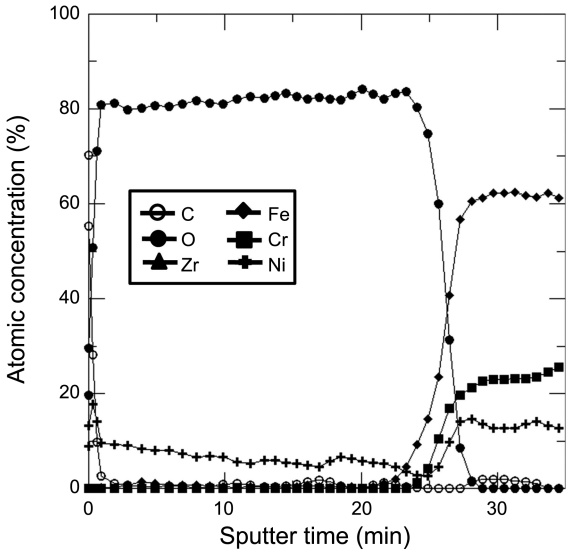

(a) 10 wt %

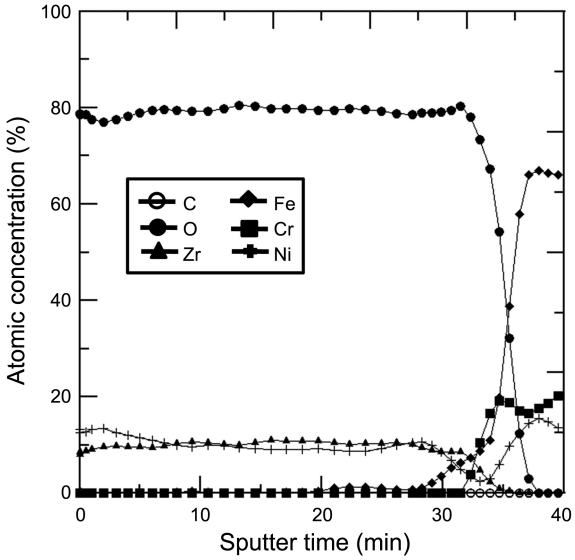

(b) 20 wt %

Figure 2. Composition profiles of the NiO-YSZ coated 316L stainless steel surface obtained from AES depth profiling. (a) NiO-YSZ film with 10 wt % Ni (b) NiO-YSZ film with 20 wt % Ni.

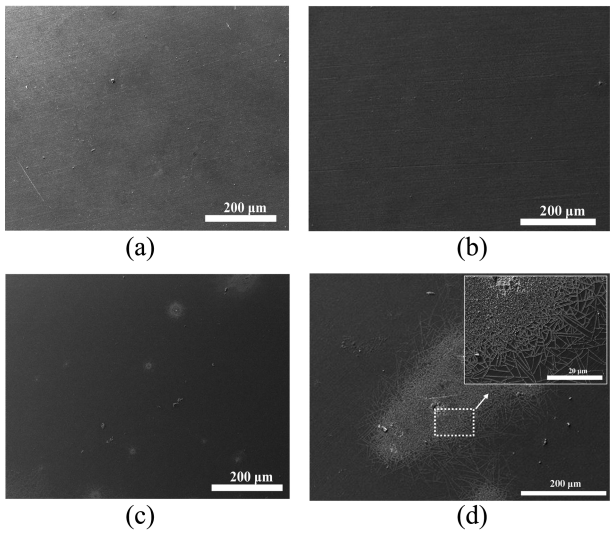

Figure 3. The SEM micrographs of NiO-YSZ coated 316L stainless steel with different Ni contents. (a) 0 wt %, (b) 15 wt %, (c) 20 wt %, (d) 25 wt %.

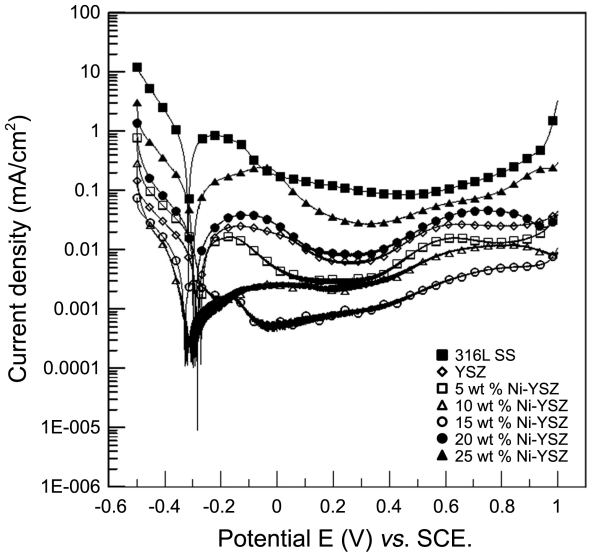

Figure 4. Potentiodynamic curves of bare 316L stainless steel and the same steel with NiO-YSZ coating with different Ni contents, which were measured at 70 °C in 1 M H_2SO_4 + 2 ppm F^- solution.

the film appears to be the different film thickness after the sol-gel coating, which is strongly affected by the viscosity of the solution during dip coating. The Ni content in the precursor used for dip-coating determines the viscosity of the solution and a thicker film induces stress during cooling when the thermal expansion coefficients of the two bonded layers are different.[12] This is supported by the measured viscosity of the solution, which was increased from 12cP to 16cP by changing the Ni content from 15 wt % to 25 wt %. The generation of the microcracks on the NiO-YSZ film was closely related to the thickness of the NiO-YSZ film on the 316L substrate.[26]

Electrochemical Properties. The corrosion resistance of NiO-YSZ coated 316L stainless steel was examined by analyzing the polarization behavior. Figure 4 shows the potentiodynamic curve obtained in the simulated PEMFC operating condition. The potentiodynamic tests were carried out at 70 °C in 1M H_2SO_4 + 2 ppm F^- solution. The polarization curves exhibited active, passive and transpassive states of corrosion and significant influence on the corrosion behavior was observed after coating. The current density at the anode potential (–0.1 V) was compared as a function of the Ni content in the NiO-YSZ film (Fig. 5). This potential is in the passive region for all the specimens compared in this study. The figure shows that the current density decreases to 15 wt % NiO-YSZ and increases again beyond 15 wt % of NiO. The minimum current density in the figure shows that the amount of current associated during corrosion can be reduced by more than two orders of magnitude compared to bare 316L stainless steel. The decrease in current density up

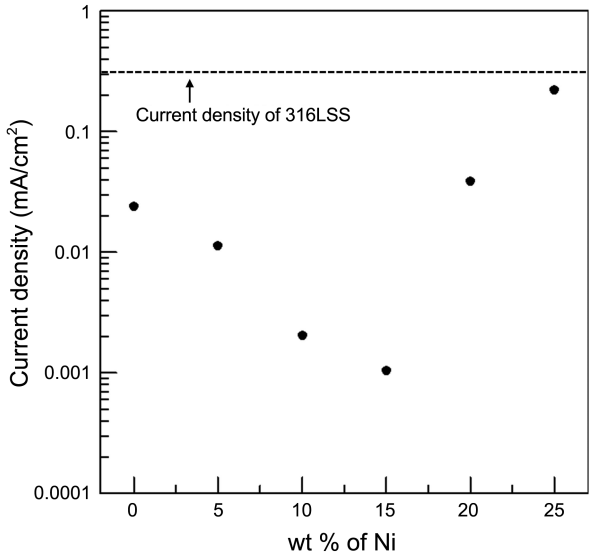

Figure 5. The current density at the anode potential (–0.1 V) as a function of the Ni content in the NiO-YSZ film. A dashed line is the current density of 316L stainless steel at the anode potential.

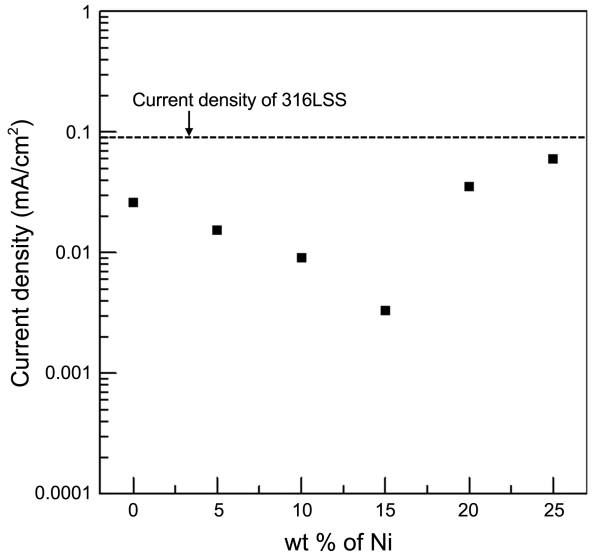

Figure 6. The current density at the cathode potential (0.6 V) as a function of the Ni content in the NiO-YSZ film. A dashed line is the current density of 316L stainless steel at the cathode potential.

to 15% NiO appears to be caused by the increase in film thickness with the Ni content that increases the viscosity of the precursors during the sol-gel coating. Another possible cause of the current decrease is the increase in passive films facilitated by NiO. A similar result was reported by Kosacki *et al.* in the case of corrosion by a solution containing sulfuric acid.[27] On the other hand, the rapid increase in current density in the specimen coated with more than 15 wt % NiO in YSZ was attributed to microcracks generated on the film, as shown in Figure 3. A similar result was also observed in the current density at the cathode potential (0.6 V). Figure 6 shows the current density of the NiO-YSZ film at the cathode potential as a function of the Ni content. The minimum current density was observed at 15% Ni in the NiO-YSZ film. The decrease in current density was also attributed to the thickness change, and the sudden increase at higher NiO contents are due to microcracks produced in the thick NiO-YSZ film.

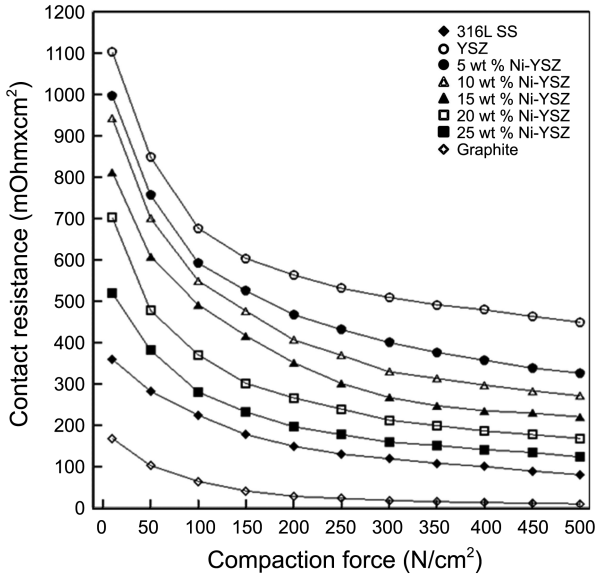

Figure 7. The interfacial contact resistance (ICR) of the specimens with and without NiO-YSZ coating as a function of the compaction force.

The corrosion parameters of the bare and 15% NiO-YSZ coated specimens were calculated from the polarization curves obtained from the potentiodynamic test. The polarization resistance (R_p) was obtained using the linear polarization method, which was found to be inversely proportional to the corrosion rate from the equation; $R_p = \beta_a\beta_c/2.3i_{corr}(\beta_a + \beta_c)$,[28] where β_a, β_c, and i_{corr} are cathodic and anodic Tafel constants and corrosion rate, respectively. Table 2 lists the corrosion parameters obtained from the polarization curves in Figure 4. The corrosion resistance (R_p) and corrosion rate (i_{corr}) of the 15 wt % NiO-YSZ-coated 316L stainless steel under PEMFC conditions were approximately 45 times and 25 times smaller than those from the bare

Table 2. Polarization resistance (R_p) and Tafel constants of bare 316L stainless steel and 316L stainless steel coated with NiO-YSZ contaiing 15 wt % Ni

	E_{corr} (mV)	i_{corr} (μA/cm^2)	β_a (mV)	β_c (mV)	R_p	Corrosion rate (mmpy)
Bare 316L stainless steel	–288.36	21.53	30.1	17.1	288.32	1.642×10^{-2}
316L stainless steel coated with NiO-YSZ containing 15 wt % Ni	–330.79	0.85	37.8	19.2	1.3×10^4	0.429×10^{-3}

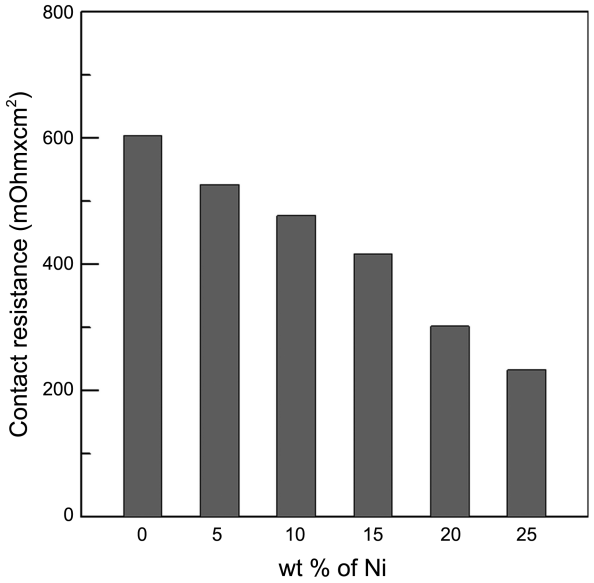

Figure 8. The interfacial contact resistance (ICR) of the NiO-YSZ film at 150 N plotted as a function of the Ni content.

stainless steel, respectively.

ICR of NiO-YSZ Film. The ICR of the bare and NiO-YSZ coated 316L stainless steel was measured as a function of the compaction force. This is because the contact resistance of the bipolar plate with the gas diffusion layer and current collector affects the power density of the PEMFC. Therefore, the change in ICR after surface modification needs to be examined in detail under a proper compaction force. Figure 7 shows the ICR of the specimens with and without the NiO-YSZ coating as a function of the compaction force. The ICR of the graphite plate was also included in the figure for comparison. The ICR values decreased with increasing compaction force due to increased contact areas, which serve as electrical junctions.[29] In contrast to the maximum corrosion resistance of the 15 wt % NiO-YSZ film, the ICR showed a minimum at 25% NiO-YSZ, indicating that the Ni content in the NiO-YSZ film strongly affects the ICR and the microcracks on the film have little effect on the area of contact junctions. This is consistent with the results reported by Marinsek *et al.*[30] They showed that the electrical conductivity of the coating layer by the sol-gel method was increased by increasing the Ni content in the YSZ precursor. The electrical conductivity measured using the four-point probe method also supports the ICR decrease by Ni addition.[31] They reported that the electrical conductivity of 316L, NiO-YSZ, and YSZ was 1.4×10^4, 5×10^2, and 4.3×10^{-2} S/cm, respectively, indicating a significant increase in electrical conductivity by introducing NiO into YSZ.

The ICR was plotted as a function of the Ni content in the NiO-YSZ film at 150 N, which is similar to the compaction force applied in a commercial PEMFC stack. Figure 8 shows that the ICR decreases linearly with increasing Ni content, suggesting that the NiO phase increases the electrical conductivity of YSZ. The minimum ICR obtained from the NiO-YSZ films at 25% Ni (233 mΩ·cm^2) was slightly higher than that of bare 316L stainless steel (174 mΩ·cm^2). In the case of the best corrosion resistance was observed with 15 wt % NiO-YSZ (ICR ~410 mΩ·cm^2). This suggests that the ICR of the coating needs to be decreased further by carful facilitation of other stress relieving ingredients in the precursor to overcome the stress induced microcracks on the thick NiO-YSZ films with low ICR values. On the other hand, the NiO-YSZ coating on the stainless steel plate shed light on the possibility of improving the lifetime of the metallic bipolar plate while minimizing the contact resistance for increasing the power density of the PEMFC by a non-metallic coating using a sol-gel method.

Conclusions

NiO-YSZ was coated on the surface of 316L stainless steel using a sol-gel method to improve the corrosion resistance and interfacial contact resistance.

1. When small amounts of Ni (from 0 to 15 wt %) were added to the precursor, the film was formed uniformly. On the other hand, films with more than 15 wt % Ni showed microcracks on the surface.

2. Potentiodynamic tests, carried out in under simulated PEMFC operation conditions in a 1 M H_2SO_4 + 2 ppm F^- solution at 70 °C, showed that the current density of the NiO-YSZ coated stainless steel was one order of magnitude lower than that of the bare stainless steel, suggesting significant improvement in corrosion resistance due to the NiO-YSZ coating.

3. Because of the NiO in the YSZ film, the interfacial contact resistance decreased as a function of the Ni content. On the other hand, the film showed higher interfacial contact resistance than bare 316L, indicating that other stress relieving ingredients will be needed in the precursor to overcome the stress induced microcracks on the thick NiO-YSZ films to achieve lower ICR values.

Acknowledgments. This work was supported by the Korea Science and Engineering Foundation (KOSEF) through the National Research Lab. Program funded by the Ministry of Science and Technology (N. R0A-2007-000-10011-0). This study was partly supported by a Korea University Grant.

References

1. Vielstich, W.; Gasteiger, H. A.; Lamm, A. *Handbook of Fuel Cells-Fundamentals*; Technology and Applications **2003**, vol. *3*, Chapter 23.
2. Tawfik, H.; Hung, Y.; Mahajan, D. *J. Power Sources* **2007**, *163*, 755-767.
3. Wang, H.; Sweikar, M. A.; Turner, J. A. *J. Power Sources* **2003**, *115*, 243-251.
4. Wang, H.; Turner, J. A. *J. Power Sources* **2004**, *128*, 193-200.
5. Cunningham, B. D.; Huang, J.; Baird, D. G. *International Materials Reviews* **2007**, *52*, 1-13.
6. Davies, D. P.; Adcock, P. L.; Turpin, M.; Rowen, S. J. *J. Appl. Electrochem.* **2000**, *30*, 101-105.

7. Metha, V.; Cooper, J. S. *J. Power Sources* **2003**, *114*, 32-53.
8. Wang, H.; Sweikar, M. A.; Turner, J. A. *J. Power Sources* **2003**, *115*, 243-251.
9. Pathan, H. M.; Min, S. K.; Jung, K. D.; Joo, O. S. *Electrochem. Commun.* **2006**, *8*, 273-278.
10. Cho, K. H.; Lee, W. G.; Lee, S. B.; Jang, H. *J. Power Sources* **2008**, *178*, 671-676.
11. Lee, S. B.; Cho, K. H.; Lee, W. G.; Jang, H. *J. Power Sources* **2009**, *187*, 318-323.
12. Munoz, M. C.; Gallego, S.; Beltran, J. I. *J. Cerda, Surf. Sci. Rep.* **2006**, *61*, 303-344.
13. Mennig, M.; Schelle, C.; Duran, A.; Damborenea, J. J.; Guglielmi, M.; Brusatin, G. *J. Sol-Gel Sci. Technol.* **1998**, *13*, 717-722.
14. Duran, A.; Castro, Y.; Aparicio, M.; Conde, A.; de Damborenea, J. J. *Inter. Mate. Rev.* **2007**, *52*, 175-192.
15. Atik, M.; Kha, C. R.; Delimaneto, P.; Avaca, L. A.; Aegerter, M. A.; Zarzycki, J. *J. Mater. Sci. Lett.* **1995**, *14*, 178.
16. Ono, S.; Nishi, Y. *J. Am. Ceram. Soc.* **2001**, *84*, 3054-3056.
17. Thomas, H.; Stefan, S.; Bernd, O. *Surf. Coat. Technol*. **2006**, *201*, 487-491.
18. Lee, W. G.; Cho, K. H.; Lee, S. B.; Park, S. B.; Jang, H. *J. Alloy. Comp.* **2009**, *474*, 268-272.
19. Dislich, H. *Sol-Gel Technology for Thin Films, Fibers, Performs, Electronics and Specialty Shapes*; Klein, L. C., Ed.; Noyes Oublications: Park Ridge, NJ 1988; p 50.
20. Dimaggio, R.; Fedrizzi, L.; Rossi, S.; Scardi, P. *Thin Solid Films* **1996**, *286*, 127.
21. Dominguez Crespo, M. A.; Garcia Murillo, A.; Torres-Huerta, A. M.; Yanez-Zamora, C.; de. J. Carrillo-Romo, F. *J. Alloy. Comp.* **2009**, *483*, 437-441.
22. Dawson, D. K.; Creamer, R. H. *Brit. J. Appl. Phys.* **1965**, *16*, 1643-1647.
23. Srdic, V. V.; Omorjan, R. P. *Ceram. Inter.* **2001**, *27*, 859-863.
24. Mondal, P.; Klein, A.; Jaegermann, W.; Hahn, H. *Solid State Ionics* **1999**, *118*, 331.
25. Hirano, M.; Watanabe, S.; Kato, E. *J. Am. Ceram. Soc.* **1999**, *82*, 2861.
26. Rivera, A.; Santamaria, J.; Leon, C. *Appl. Phys. Lett*. **2001**, *78*, 610-612.
27. Kosacki, I.; Suzuki, T.; Prtrovsky, V.; Anderson, H. U. *Solid State Ionics* **2000**, *136*, 1225.
28. Jang, H. J.; Park, C. J.; Kwon, H. S. *Electrochimica Acta* **2005**, *50*, 3503-3508.
29. Zhou, P.; Wu, C. W.; Ma, G. J. *J. Power Sources* **2006**, *159*, 1115-1122.
30. Marinsek, M.; Pejovnik, S.; Macek, J. *J. Euro. Ceram. Soc.* **2007**, *27*, 959-964.
31. Esfakur Rahman, A. H. M.; Kim, J. H.; Lee, K. H.; Lee, B. T. *Surf. Coat. Technol*. **2008**, *202*, 2182-2188.